Sensors & Transducers, Vol. 157, Issue 10, October 2013, pp. 428-433

www.sensorsportal.com

Sensors & Transducers

http://www.sensorsportal.com

Research of Water Hazard Detection Based on Color and Texture Features

[1] Yibing ZHAO, [2] Yunxiang DENG, [3] Chi PAN, [4] Lie GUO
[1] Department of Vehicle Engineering, State Key Laboratory of Structural Analysis for Industrial Equipment, Dalian University of Technology, Dalian 116024, China
[2] School of Management, Dalian Jiaotong University, Dalian 116028, China
[1] E-mail: zhaoyibing005@163.com

Received: 27 October 2013 /Accepted: 30 October 2013 /Published: 31 October 2013

Abstract: In this paper, we focus on the need for water hazard detection based on the characteristics of the static water body in off-road environment, which includes three main sections: extraction of color and texture features, building SVM model and practical detection of water bodies. Based on the features of high intensity, low saturation and low texture of the water bodies existed in off-road environment. Saturation-value ratio feature extracted from hsv color space of water body region, combined with other four texture features conducted by gray level co-occurrence matrix constitute the five-feature vector. Training set is established from sample images after the images are well preprocessed. Then build the svm model based on the training set. Our task is to separate practical samples into two classes: water region and land region according to the predict result calculate by svm model. Experimental results demonstrate significant progress on detection of water body hazard in off-road environment, which effectively reduce the influence of illumination variation exert on detection when only using color feature to detect. *Copyright © 2013 IFSA.*

Keywords: Computer image processing, HSV color space, Texture, Gray level co-occurrence matrix, SVM support vector machine.

1. Introduction

Water hazard is one of the most challenging obstacles in off-road environments. The failure detection of the water hazard by UGV (Unmanned Ground Vehicle) could cause a deep trap in the hazard, which could damage the electronics of UGV [1]. Both passive sensors and active sensors have been explored for water detection [2]. Active sensors often get no return value on free-still water, which has excellent effect on water detection. Furthermore, fusing information of active sensor and passive sensor could make water hazard more detectable [3, 4]. But, it could be desirable for UGVs to work without emitting detectable electromagnetic signals when executing military operation [2]. Stereo range data use to analyze patterns consistent with range reflections. The stereo range data on terrain reflection dominated region below the ground surface [1]. While, there may be little stereo range data on water hazard because the surface of water bodies lack texture generally, particularly when they are stationary [5]. Polarization cameras have been proved quite appropriate on water detection by several researchers [6]. However, the price of polarization cameras, the sane as SWIR, TIR and hyper spectral sensors, are relatively higher compared with visible sensors [7]. Consequently, passive perception solution, such as industrial color cameras, is more desirable for water hazard detection [8].

Article number P_RP_0002

Water body hazard in outdoor environment tend to appears higher brightness, lower saturation and lower texture than terrain around comparatively. In this paper, we focus on the research of the characters listed above. Fusion of saturation-value ratio [2] color feature extracted from hsv color space and other four texture features: Asm, Ent, Con and Cor, conducted from gray level co-occurrence matrix are addressing in our experiments. Details of our multi-cue detector are discussed in the later section. We will analyze the color information and the texture information in detail and concerning the way we extract them in section 2. While in section 3, we will discuss the fundamental information and kernel type of SVM-Support Vector Machine. Experiment results will be listed in section 4 though a set of figures with contour of detected water body hazard labeled on image.

2. Water Features Analysis

2.1. Color Cue of Water

HSV model represent color with hue, saturation and value in an attempt to be more intuitive and perceptually relevant than the RGB model described by Cartesian (cube) representation. Thus this HSV representation is widely utilized in computer graphical field. Hue is color attribute, which indicates frequency location of color in the spectrum; saturation describes the degree of departure of a color sensation from that of a white or gray; value represents the degree of intensity of the light. Equation (1) used to achieve the transformation between RGB and HSV color space.

$$\begin{cases} V = \frac{1}{3}\left(R+G+B\right) \\ S = 1 - \frac{3}{R+G+B}\left[\min(R,G,B)\right] \\ H = \arccos\left\{ \frac{\left[(R-G)+(R-B)\right]/2}{\sqrt{\left[(R-G)^2+(R-B)(G-B)\right]}} \right\} \end{cases} \tag{1}$$

As free stationary water hazard reflect most of the incident light, reflection appears on the surface of the water could be a common characteristic. Reflection could be divided into two cases: the reflection of the sky dominates and the terrain reflection dominates. In this paper, we concentrate on the latter issue.

When most surface of the water reflects the scene of the sky, water region with reflection of sky can easily discriminated from the other terrain by brightness. Without shelter and reflection from terrain around, water shows a higher brightness than the terrain. Because water reflects colour of the sky, meanwhile the average brightness of the sky is much higher than the mean brightness of the terrain. Thus, the average brightness of water where it reflects the sky is mid-way between that of the sky and the terrain. Nevertheless, water still possesses a relatively high brightness than terrain [8].

The other characteristic that water hazard presents usually is low saturation, while vegetation of terrain around is saturated generally. We focus on this characteristic to detect water hazard, for it is more probable for a region with low saturation proved to be water hazard than a saturated region [9].

A. L. Rankin [2] recently performed a survey of ratio of saturation and brightness and algorithms applicable to water detection. In this work, portion of the water regions with sky reflection was manually segmented. The hue, saturation, and value levels of these regions are plotted in Fig. 1. As illustrate in Fig. 1(a), hue level of the water region with sky reflection can cover the full hue spectrum, which means it is of marginal use for water region detection. According to our sufficient statistic about saturation and value levels of water region and terrain region respectively, as shown in Fig. 1(b), water region cluster in the high brightness, low saturation region. Meanwhile, a ray from the origin, represents the ratio of the saturation and value, separates the scatters stands for the characteristic of water region (orange scatters) and terrain region (purple region) practically. Therefore, we consider that ratio to be the colour-based cue to detect water region contains sky reflection. Fig. 1(d) shows the segmentation using the saturation-value ratio on the image of Fig. 1(c). Note that saturation-value ratio could be selected to detect water region with reflection of sky for most of the water region in Fig. 1(c) is segmented under this colour cue.

2.2. Texture Cue of Water

It is obviously that although color cue performs satisfactorily in experiment we introduced above, formulating a single cue, especially color cue, capable for detect water region in different situation is still a big challenge. The color features of water vary with the changing of ambient light condition. Thus low texture could be another cue of water region. R. M. Haralick proposed conception of gray level co-occurrence matrix, who applied the theory in image classification primarily. This technology has been widely used in field of image texture analysis and become an important way to research texture characteristic from image [10].

Gray level co-occurrence matrix (GLCM) is defined to describe the relative frequencies with which a pair of pixels separated by a specified distance occurs on the image under a fixed angle. It presents as $P_d(i,j)(i,j=0,1,2,3,\ldots\ldots L-1)$, where L means image gray level; i, j are two pixels gray level; d means the fixed displacement vector. Generally, orientation θ are 0°, 45°, 90° and 135°. As shown in figure 2. Each element $P_d(i,j)$ in GLCM represents the relative frequency of which two pixels of gray level i, j appears under relative position (dx, dy).

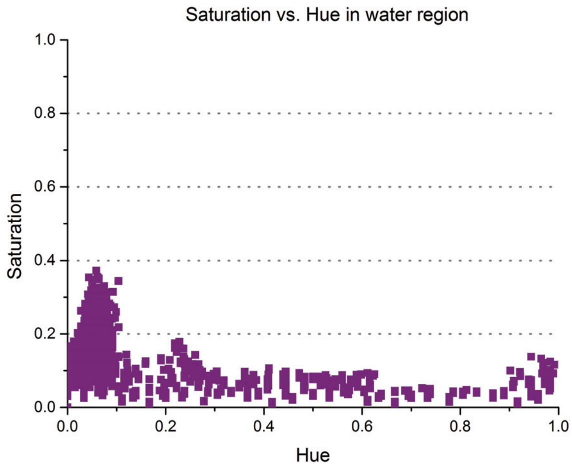

(a)

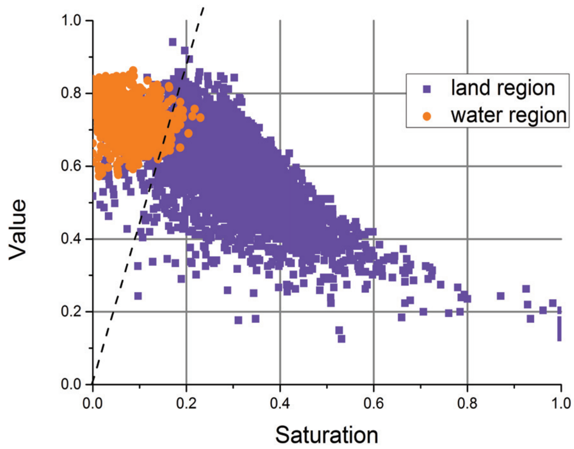

(b)

(c)

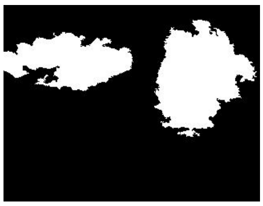

(d)

Fig. 1. Statistical analysis of saturation, value and hue of water and terrain region: (a) Saturation and Hue level of water region with sky reflection; (b) saturation and value in water region (orange) and terrain (purple) region respectively; (c) practical water hazard image with reflction of sky; (d) detect water region with s/v ratio.

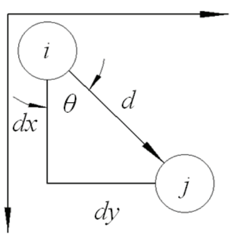

(a) Pixel pair.

$$
\begin{bmatrix}
P_d(0,0) & P_d(0,1) & \dots & P_d(0,j) & \dots & P_d(0,L-1) \\
P_d(1,0) & P_d(1,1) & \dots & P_d(1,j) & \dots & P_d(1,L-1) \\
\dots & \dots & \dots & \dots & \dots & \dots \\
P_d(i,0) & P_d(i,1) & \dots & P_d(i,j) & \dots & P_d(i,L-1) \\
\dots & \dots & \dots & \dots & \dots & \dots \\
P_d(L-1,0) & P_d(L-1,1) & \dots & P_d(L-1,j) & \dots & P_d(L-1,L-1)
\end{bmatrix}
$$

(b) Gray-level co-occurrence matrix

Fig. 2. Representation of pixel pair in gray-level co-occurrence matrix.

Among fourteen textural statistical features extracted from GLCM, four of them are uncorrelated proved by Ulaby et al [11]. Properties of these four features: ASM, Ent, Con and Cor are discussed below.

1) ASM (angular second moment): also called energy. High energy means the gray level distribution form is constant or periodic.

$$\text{ASM} = \sum_{\mathrm{i}=0}^{L-1}\sum_{\mathrm{j}=0}^{L-1} P_d(i,j)^2 \tag{2}$$

2) Ent (entropy): measures the disorder or complexity of an image. Low entropy means the image is texturally uniform or texturally simple.

$$\text{Ent} = -\sum_{i=0}^{L-1}\sum_{j=0}^{L-1} P_d(i,j)\, logP_d(i,j) \tag{3}$$

3) Con (contrast): measures the amount of local variations of the image. Low contrast image presents a low spatial frequency feature in an image.

$$\text{Con} = \sum_{\mathrm{i}=0}^{L-1}\sum_{\mathrm{j}=0}^{L-1} (\mathrm{i}-\mathrm{j})^2\, P_d(\mathrm{i},\mathrm{j}) \tag{4}$$

4) Cor (correlation): measures linear dependencies of gray level. A higher correlation shows more homogeneous in the specified orientation.

$$\text{Cor} = \frac{\left(\sum_{i=0}^{L-1}\sum_{j=0}^{L-1} ijP_d(i,j) - u_x u_y\right)}{\delta_x \delta_y} \tag{5}$$

where

$$u_x = \sum_{i=0}^{L-1} i \sum_{j=0}^{L-1} Pd(i,j),\quad u_y = \sum_{j=0}^{L-1} j \sum_{i=0}^{L-1} Pd(i,j)$$

$$\delta_x = \sum_{i=0}^{L-1}(i-u_x)\sum_{j=0}^{L-1} P_d(i,j),\quad \delta_y = \sum_{j=0}^{L-1}(i-u_y)\sum_{i=0}^{L-1} P_d(i,j)$$

2.3. Color and Textures Features Extraction

We notice the fact that textural characteristic of water and terrain region in off-road environment do not indicate strong cue of orientation. Thus, for each feature, the average of the feature under four orientations is applied as the corresponding textural statistical features in order to reduce the computational complexity. We prepare several sample image sets for our work. In our work, we segment water body hazard region from the image and separate image into 8×8 sized sub blocks. After that we transform the image from RGB color model to HSV model to obtain saturation-value ratio color features from each sub block and extract texture statistical features calculate from GLCM of each sub block after gray level of the image has been compressed form 256 to 16, also for reducing computational complexity. Texture features and color feature are combined as a 5-D feature vector: $\upsilon = (\mathrm{Asm}, \mathrm{Ent}, \mathrm{Con}, \mathrm{Cor}, \mathrm{S/V})$. We collect three image sample sets to analyze. Statistical result of features extracted from water region and terrain region shown in Table 1.

Table 1. Five features extracted from sample image.

	Asm	Ent	Con	Cor	S/V
Water	0.3470	1.4892	0.2554	1.5171	0. 1402
	0.1265	0.7940	0.8948	2.5243	0. 2815
	0.2484	1.0427	0.6755	3.0314	0. 1517
Terrain	0.0377	2.4564	1.2319	0.6116	0.5860
	0.0868	3.3245	1.6472	0.2670	0.6524
	0.0499	1.9083	2.0469	0.4724	0.4727

We focus on the features distance between the two –class by analyze the Table 1. The ASM and the Cor of water region higher than that of terrain region, while Ent and Con is lower. What's more the s/v ratio feature of water is obviously under the relative feature of terrain. These analysis results consistent with the theory we introduced ahead.

3. SVM-Support Vector Machine

3.1. SVM Fundamental

Support vector machines (SVM) are based on the principle of structural risk minimization (SRM), derived from statistical learning theory developed by Vapnik [12]. SVM has stronger capability of generalization compared with existing machine learning algorithm especially when number of samples is quite infinite. What's more, SVM possesses the capability to process high dimension and nonlinear problem.

SVM method was originally designed for linearly separable classes of samples classification. Its purpose is to finds the hyperplane with the maximum margin between two- class of samples. The hyperplane is defined by $w^T x + b = 0$, where w is normal to the hyperplane. The training data should satisfy the following constraints as (6):

$$y_i(w^T x_i + b) - 1 \geq 0,\ i = 1, 2, ..., n \tag{6}$$

Therefore the hyperplane which optimally separates the samples minimizes (7):

$$\Phi(w) = \min\ \frac{1}{2}\|w\|^2 \tag{7}$$

It is convenient to construct a Lagrangian function of the problem to solve constrained minimization problems defined by Eq. (6) and Eq. (7)

$$L(w,b,\alpha) = \frac{1}{2} w^T w - \sum_{i=1}^{n} \alpha_i [y_i (w^T x_i + b) - 1], \tag{8}$$

where α are the Lagrange multipliers. The Lagrangian must be minimized with respect to w, b and maximized with respect to $\alpha \geq 0$.

3.2. SVM Kernel Function

When it is difficult for linear SVM classification algorithm to find an optimal hyperplane in a lower feature space, we use kernel functions to extend input features mapping into a higher dimension of feature space where SVM could perform a linear classification. Here are three widely used kernel mapping functions.

Polynomial kernel function:

$$K(x, x') = \left(\langle x, x' \rangle + 1\right)^d$$

RBF kernel function:

$$K(x, x') = \exp\left\{-\gamma \|x - x'\|^2\right\}, \gamma > 0$$

Sigmoid kernel function:

$$K(x, x') = \tanh(v\langle x, x'\rangle + c)$$

Among the three kernel function, RBF kernel converge on a wide range and compute fast with fewer parameter. SVM with RBF kernel function performs well for it possess relative high prediction accuracy without increasing calculating complexity. Thus, in our work we choose RBF kernel function to mapping input feature space into higher dimension which will be introduced in section 4.

4. Experiment Result

In our work, a platform based on our own UGV is operated to collect image with water hazard, with resolution of 320×240. Image process platform constructed by computer containing an AMD 2.0 GHz processor. Libsvm package developed by Chih-Jen Lin in Taiwan University applied to build SVM model with default parameters and separate water from sample images.

The number image is divided into sub-blocks, and each sub-block size affects the dimension of the feature matrix, thereby affecting the water consumed by the time the obstacle detection accuracy and detection. In order to find that size of sub-block satisfies both detection accuracy and the time it takes to detect. We try to segment image with different size of blocks and extract features from them in each experiment. As shown in Fig. 3, size of sub-block impacts on the training time and predict time consumption directly, as well as the mean accuracy of prediction. Better prediction would be achieved when sample capacity goes larger, which means image segmented by tinier blocks. However, training becomes quite complex when image segmented into too small sub-blocks, which leads a high consumption of training and prediction time and a low predict accuracy. Larger sub-block would bring us a quick training and prediction process, while quite low prediction accuracy would be unsatisfied. In this paper, we use sub-block with size 8, for seek a relative high prediction accuracy over a short processing time.

When it is difficult for linear SVM classification algorithm to find an optimal hyperplane in a lower feature space, we use kernel functions to extend input features mapping into a higher dimension of feature space where SVM could perform a linear classification. In our work, we segment image into different size of sub-block, train these sample set using SVM with polynomial kernel function and RBF kernel function respectively. As shown in Fig. 4, SVM with RBF kernel function performs well for it possess relative high prediction accuracy without increasing calculating complexity. Thus, in our work we choose RBF kernel function to mapping input feature space into higher dimension.

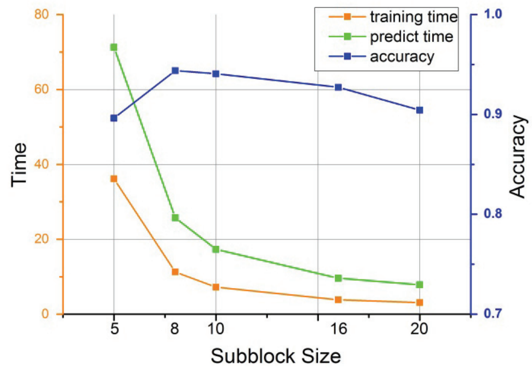

Fig. 3. Training, predict time and accuracy under different size of block.

In our work, we extract features from several sets of preprocessed images and train the normalized feature matrix to form a satisfied SVM model. Large amount of images a test in our work, the accuracy of this method achieves 96.2 % (accuracy means the ratio between tested region and the practical region). As shown in Fig. 5, the method we applied in this paper achieves a satisfied result. The figure illustrate that, the contour of the water hazard is labeled in the result image by conducting the detection method we proposed in this paper. And the contour can depict the shape of the water obstacle accurately.

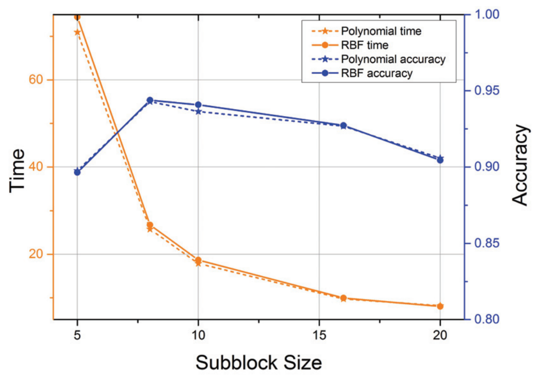

Fig. 4. Polynomial vs. RBF on time consumption and accuracy.

5. Conclusions

In this paper, we have summarized an approach of water hazard detection in off-road environment using passive sensors. A multi-cue water detector fuses the feature from water color and texture.

In addition to the obstacle, especially water reflects the characteristics of high brightness; it also reflects the low saturation characteristics. Utilization ratio of saturation and brightness characteristics, combined from GLCM texture features extracted. Detecting the obstacle so that the water more efficiently. Compared with the previous water detector using single feature, this method is robust to variation of ambient lightness.

Fig. 5. Performance of the method to detect water body hazard.

This paper studies the image into sub-block size, through multiple sets of comparative tests and found the sub-block size on the water obstacle the relationship between detection accuracy and time consuming. Select to satisfied the detection accuracy without excessive increase characteristic dimension block size for the test. Meanwhile, in a low-dimensional space cannot be classified, considering the use of kernel function of the input feature space up to high-dimensional space, in high-dimensional space using SVM classification, this paper we consider various kernel function method at elevated dimension and effects of different contrasts RBF kernel and polynomial kernel function, investigated their detection accuracy and experimental aspects of the merits of time consuming, select the appropriate kernel function to increase dimension of the feature space.

Because the water hazard in wide-open environment often appears with reflection from terrain around, it is still hard for our method to identify terrain reflection from the water region. In future work, we will focus on another features of water that are more robust performing in out-door environment water detection and improve the autonomous environment perception and obstacle avoiding ability.

Acknowledgements

The research work was supported by National Natural Science Foundation of China under Grant No. 51205038, Specialized Research Fund for the Doctoral Program of Higher Education under Grant No. 20110041120024 and the Fundamental Research Funds for the Central Universities under Grant No. DUT13JS14 and DUT13JS02.

References

[1]. Rankin, A., and L. Matthies., Daytime water detection and localization for unmanned ground vehicle autonomous navigation., in *Proceedings of the 25th Army Science Conference*, 2006.

[2]. Rankin, Arturo, and Larry Matthies., Daytime water detection based on color variation., in *Proceedings of the IEEE/RSJ International Conference on Intelligent Robots and Systems (IROS),* 2010.

[3]. Rankin, Arturo L., Larry H. Matthies, and Andres Huertas. Daytime water detection by fusing multiple cues for autonomous off-road navigation. *Jet Propulsion Laboratory,* Pasadena CA, 2004.

[4]. Yao, Tuozhong, et al., Multi-feature fusion based outdoor water hazards detection., in *Proceedings of the IEEE International Conference on Mechatronics and Automation (ICMA'07),* 2007.

[5]. Rankin, Arturo, Tonislav Ivanov, and Shane Brennan, Evaluating the performance of unmanned ground vehicle water detection., in *Proceedings of the 10th Performance Metrics for Intelligent Systems Workshop*, 2010.

[6]. Qin Ling, Mechanism research on water obstacle detection based on the polarization information, *Nanjing University of Science and Technology,* 2009.

[7]. Rankin, Arturo L., Larry H. Matthies, and Paolo Bellutta., Daytime water detection based on sky reflections., in *Proceedings of the IEEE International Conference on Robotics and Automation (ICRA)*, 2011.

[8]. Iqbal, Mohammad, et al., A survey on outdoor water hazard detection., in *Proceedings of the 5th Intl. Conf. on Information and Communication Technology and Systems (ICTS),* 2009.

[9]. Huang Ping-Ping, Wang Jian-Hua Chen Chang-Feng, Experimental Studies of Several Reflection Detection Methods, *Microcomputer Information*, 27, 9, 2011, pp. 199-200.

[10]. Zhao, H-Y., G-M. Xu, and H. Peng., Performance Evaluation for the Algorithms to Measure Texture Coarseness, *Computer Science*, 38, 6, 2011, pp. 288-292.

[11]. Ulaby, Fawwaz T., et al., Textural information in SAR images., *IEEE Transactions on Geoscience and Remote Sensing,* 2, 1986, pp. 235-245.

[12]. Ivanciuc, Ovidiu., Applications of support vector machines in chemistry., *Reviews in Computational Chemistry*, 23, 2007, pp. 291.